Efficient proton conduction in dry nanofilms of amorphous aluminosilicate†

Yoshitaka Aoki,[a] Emi Muto,[a] Shinya Onoue,[a] Aiko Nakao[ab] and Toyoki Kunitake*[a]

Amorphous aluminosilicate nanofilms as prepared by a sol–gel process and post-annealing exhibit proton conduction at a wide temperature range in dry air with a lowest area specific resistance of 0.24 Ω cm^2 at 400 °C.

Zeolites are a class of crystalline aluminosilicates which are built up by corner-sharing SiO_4 and AlO_4 tetrahedra. They often exhibit strong Brønsted acidity, because the negative charge on the aluminosilicate framework can accommodate a large amount of proton. Hence, certain zeolite compounds give a proton conductivity of 10^{-7} S cm^{-1} (at 300 °C) even in dry atmosphere.[1,2] In spite of the potential proton conductivity, conventional zeolite compounds are not considered as practical candidates of the electrolyte membrane in fuel cells and related uses, because dry polycrystalline zeolites, even if proton conducting, will not effectively suppress permeation of fuel gases (typically hydrogen and oxygen molecules) due to their characteristic cage structures. In addition, thin film electrolytes that are fabricated from polycrystalline zeolites contain abundant grain boundaries which would facilitate diffusion of fuel gases.

This drawback may be alleviated if a dense, non-crystalline film can be produced. We have demonstrated that defect-free nanofilms of amorphous metal oxides become available by careful fabrication of nanometer-thick layers.[3] A similar approach will be applicable to formation of defect-free nanofilms of aluminosilicates. The basic covalent framework of the aluminosilicate should be maintained even in the amorphous film, exhibiting Brønsted acidity and the consequent proton conductivity. Permeation of fuel gases may be suppressed due to the absence of crystalline cage structure and grain boundaries in a dense amorphous film.

$Al_xSi_{1-x}O_{2-2/3x}$ films were prepared on an ITO substrate (Aldrich) by a multiple spin-coating of precursor solutions of tetraethoxysilane (TEOS) and aluminum tri-sec-butoxide (Al(O^{s}Bu)$_3$). The Al/Si ratio of the precursor mixture were 0/100, 5/95, 10/90, 20/80, 90/10 and 100/0, and the resulting films were denoted as S100, A5S95, A10S90, A20S80, A90S10 and A100, respectively. Calculated amounts of TEOS were added to 15 ml of 1-PrOH, and then 0.1 M hydrochloric acid was added to the mixture in the ratio of TEOS/H$_2$O = 1/2. After the mixture was vigorously stirred for 1 h at room temperature, Al(O^{s}Bu)$_3$ was added in given ratios of Al/Si, and the mixture was further stirred at 50 °C for 1 h. The solution was allowed to cool to room temperature, filtered with 0.2 µm diameter porous cellulose filter (Advantec), and diluted to 50 ml (total volume) with 1-PrOH. The final concentration of the combined metal components was 50 mM for A90S10 and A100, and 100 mM for the others. The precursor sols were spin-coated onto the ITO substrate at 3000 rpm for 40 s by a Mikasa 1H-D7 spin coater and, the as-deposited layer was thermally annealed below 400 °C. The spin-coating/annealing cycle was repeated as required.

The film morphology was characterized by scanning electron microscopy (SEM) (see ESI†). Films were formed always uniformly, covering the ITO surface without pinholes, cracks and aggregates of large particles. The thickness of $Al_xSi_{1-x}O_{2-2/3x}$ films, as determined by SEM, was in the range of 100 to 120 nm. The Al/Si ratio is greater in the corresponding thin film than in the precursor sol (Table 1). This must be caused by a greater reactivity of Al(O^{s}Bu)$_3$ relative to that of TEOS, as reported in the atomic layer deposition (ALD) process.[4] Further structural characterization was performed by cross-sectional transmission electron microscopy (TEM), showing that the $Al_xSi_{1-x}O_{2-2/3x}$ films are amorphous and are composed of a homogeneously mixed glass of alumina and silica without phase separation (Fig. 1). This result is consistent with the report that alumina and silica form glassy solid solutions in all ranges of Al/Si ratios.[5]

The electrical resistance across the film (R_{ox}) was determined by ac impedance spectroscopy. A Pt button electrode (2 mm diameter) was deposited on the film by ion sputtering to form a Pt/$Al_xSi_{1-x}O_{2-2/3x}$/ITO-stack. All the measurements were carried out after 1 h of thermal stabilization at each temperature. The obtained impedance spectra were analyzed by the nonlinear least-squares fitting with an equivalent circuit model. The area specific resistance (R_{AS}) was determined from across-the-film resistance and electrode area (S) as $S_{AS} = R_{ox}S$. The details of measurement and analysis of impedance spectra have been described elsewhere.[6]

[a]Topochemical Design Lab., Frontier Research System, Institute of Physical and Chemical Research (RIKEN), 2-1 Hirosawa, Wako, Saitama, 351-0198, Japan. E-mail: kunitake@ruby.ocn.ne.jp; Fax: +81-48-464-6391; Tel: +81-48-467-9061
[b]Surface Analysis Lab., Institute of Physical and Chemical Research (RIKEN), 2-1 Hirosawa, Wako, Saitama, 351-0198, Japan
† Electronic supplementary information (ESI) available: SEM images and complex impedance spectra. See DOI: 10.1039/b618920b

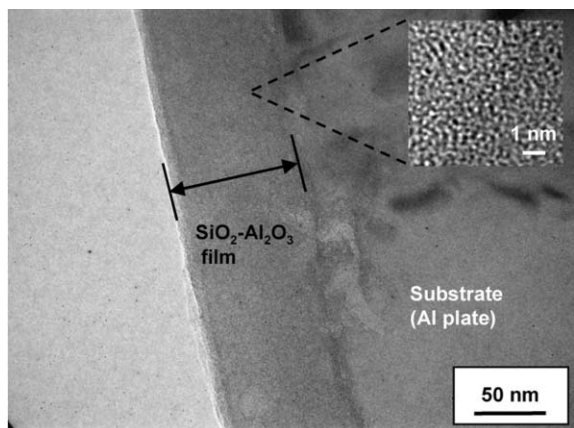**Table 1** Chemical composition, thickness and area specific resistance (R_{AS}) of amorphous aluminosilicate films

Nanofilm	Atomic ratio Al/Si		Thickness/ nm	R_{AS}/Ω cm^2 (at 80 °C in dry air)
	In precursor	In film[a]		
S100	0/1.00	0/1.00	100	1.2×10^5
A5S95	0.05/0.95	0.14/0.86	100	6.4×10^3
A10S90	0.10/0.90	0.18/0.82	120	7.5×10^2
A20S80	0.20/0.80	0.45/0.55	110	1.3×10^3
A90S10	0.90/0.10	0.92/0.08	100	$>10^6$
A100	1.00/0	1.00/0	100	$>10^6$

[a] Determined by X-ray photoelectron spectroscopy.

Fig. 1 Cross-sectional TEM image of an amorphous aluminosilicate film (A10S90) prepared on the Al metal plate. The specimen for TEM observation was prepared by using an ultramicrotome (Leica).

Fig. 2 Arrhenius plots of R_{AS} in dry air and in wet air of the $Al_xSi_{1-x}O_{2-2/3x}$ films. Symbols show the measured data and dashed lines are a guide for the eye.

The ionic conductivity of the different ceramic films was first compared under dry air atmosphere at 80 °C. The measurement was performed in a tubular furnace by purging a mixed gas of ultra-pure N_2 and O_2 at a rate of 100 ml min^{-1}. The low-Al content films A5S95, A10S90 and A20S80 exhibited small semicircles in the high frequency region and spikes in the low frequency region in Cole–Cole plots of impedance spectra (see ESI†). These features are characteristic of the assembly of an ion-conducting film and an ion-blocking electrode.[7] Thus, we conducted fitting of the spectrum with an equivalent circuit of series of system resistance (R_s), electrical components (resistance (R_{ox}) and capacitance (Q_{ox})) of film and capacitance (Q_i) due to the charge up at the interface of ion-conductive film and two electron-conductive electrodes. These results indicate that the low Al-content films are ionic conductors. The R_{AS} values (at 80 °C in dry air) are listed in Table 1. A pure silica film, S100, also shows the ionic conduction at 80 °C in dry air; however, its R_{AS} value is several orders of magnitude larger than those of the Al-doped films.

Impedance spectra of high Al-content films, A100 and A90S10, show different behavior from those of the low Al-content films. The curve simply increases with increasing frequency, and becomes a line parallel to the Z''-axis (see ESI†). This is typical of a simple electrical insulator. The R_{AS} value of the A100 and A90S10 films were calculated to be larger than 10^6 Ω cm^2 by fitting with an equivalent circuit.

Subsequently, the electrical conductivity of the better conductive films, A5S95, A10S90 and A20S80, was measured at a temperature range of 50–300 °C in dry air as well as in wet air (2% H_2O). The wet air was prepared by passing the dry air through water kept at 25 °C. Fig. 2 shows the Arrhenius plots of R_{AS} of the low Al-content films. At temperatures below 100 °C, R_{AS} in dry air is higher than that in wet air by a factor of more than 10 in all cases. Interestingly, the R_{AS} values in this temperature region give temperature dependences that are different between the dry air and wet air conditions. It is enhanced with increasing temperatures in dry air, while it decreases with temperature in wet air. Quite different behavior was observed at temperatures higher than 100 °C, and more or less linear Arrhenius plots were found. In the higher temperature region, R_{AS} decreases as temperature increases,
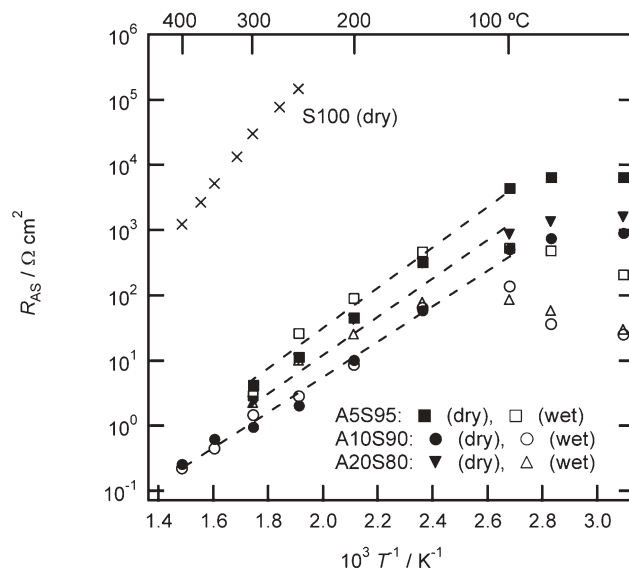
and those in dry air and in wet air become very close with each other.

Apparently, the proton transport below 100 °C is mediated predominantly by the liquid water deposited in the aluminosilicate film, and the water deposition and the consequent proton conduction is enhanced with lowering temperatures. Such effects are much smaller when dry air condition is used. In contrast, the ion transport at temperatures above 100 °C must be supported by mobile protons in the amorphous aluminosilicate, with its mobility being enhanced with increasing temperature. The A10S90 film exhibits the lowest R_{AS} of the three and the R_{AS} value at 300 °C is of the order of 10^0 Ω cm^2. The corresponding electrical conductivity is 1.0×10^{-5} S cm^{-1}. This value is higher than that of mordenite-type zeolite by a factor of 10^2.[1] Additional measurements of this sample at 350 and 400 °C gave R_{AS} values of 0.57 and 0.24 Ω cm^2, respectively. The latter value is close to R_{AS} of 0.15 Ω cm^2 that is required for the practical electrolyte membrane in commercial fuel cells.[8]

We measured the temperature dependence of R_{AS} of S100 in dry air as reference. It is increased as temperature increased from 80 to 100 °C, and the R_{AS} at 100–200 °C is larger than 10^6 Ω cm^2, being too high to be detected by the frequency analyzer. It is less than 10^6 Ω cm^2 at 250 °C or above. It is reported that dry silica gels show electrical conductivity due to migration of the native protons on silanol and exhibit values of 10^{-9}–10^{-12} S cm^{-1} at 250 °C in dry air.[9] The conductivity of the S100 film is 10^{-8}–10^{-10} S cm^{-1} at temperatures above 250 °C, and are rather close to that of the dry silica gel. The current aluminosilicate films give much greater conductivities that cannot be explained by proton hopping on silanol.

In order to test whether or not the ionic conductivity is caused by weakly-adsorbed water, the R_{AS} value was measured for an A10S90 film kept at 400 °C in dry air for different periods of time (Fig. 3). Surprisingly, R_{AS} did not change for 3 days under such conditions, and the electric leakage due to breakdown was not observed during this long-time heating. It appears that native
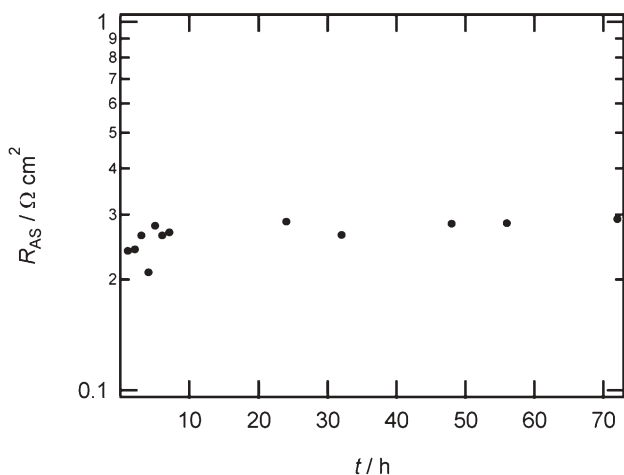
Fig. 3 The variation of R_{AS} of A10S90 film at 400 °C in dry air at different time intervals.

protons are sufficiently retained in the film up to at least 400 °C even in dry air. This conductive behavior is clearly different from those of known oxide gels and crystalline ceramics. It is reported that mixed metal oxide xerogels, such as SiO_2–P_2O_5,[10] and ZrO_2–P_2O_5,[11] reveal high proton conductivities at temperatures below 150 °C in wet atmosphere due to the presence of water incorporated in the xerogel. The latter compounds, however, exhibit quick deterioration of protonic conductivity due to loss of water at elevated temperatures or under dry atmosphere. Another reported example of proton-conducting ceramics is crystalline $BaCe_{0.8}Y_{0.2}O_{3-\delta}$, which reveals effective protonic conduction under hydrogen or wet atmospheres. The protonic carrier in this case is apparently formed by the reaction between oxygen lattice defects and moisture as follows:[12] $(H_2O)_{gas} + V_O^{\cdot\cdot} + O_O^x \leftrightarrow 2\ OH_O^{\cdot}$ It is reported that aluminosilicate glass shows strong acidity due to the presence of Brønsted acid sites composed of the OH group bridging Al and Si atoms.[13] Bronnimann *et al.* reported that the OH group in silicate compounds can be maintained after heating at 500 °C.[14] Therefore, the high-temperature protonic conduction of our aluminosilicate films appears to be supported by proton migration on Brønsted sites in the amorphous framework.

In terms of area specific resistance, the amorphous aluminosilicate films is not inferior to polycrystalline ceramic films. Kosacki and Anderson prepared nanocrystalline $SrCe_{0.95}Yb_{0.05}O_{3-\delta}$ thin film of 1 μm thickness on Al_2O_3 substrate by spin-coating of polymer precursors, and reported that its protonic conductivity was 10^3 times higher than that of the bulk sample due to the enhanced conductivity at grain boundaries.[15] The R_{AS} at 400 °C of this film along the thickness direction is calculated to be about 0.07 $\Omega\ cm^2$ from the conductivity data. Recently, Ito *et al.* reported that a 700 nm-thick $BaCe_{0.8}Y_{0.2}O_{3-\delta}$ membrane showed promising performance as a proton-conducting electrolyte of a fuel cell.[16] The R_{as} value of this film (0.12 $\Omega\ cm^2$ at 400 °C) is comparable to that of our A10S90 film (0.24 $\Omega\ cm^2$, 400 °C). The conductivity of the aluminosilicate film may be further improved by elaboration of chemical composition, texture and thickness, and its use as an ultrathin solid ionic materials will facilitate versatile applications. The class of ceramic nanofilms as prepared by the current spin coating method has been found to be self-supporting.[17] Therefore, the aluminosilicate films in the current study can remain intact when placed on porous substrates. Their potential as electrolyte membranes is being examined in our laboratories.

Notes and references

1 T. Hibino, T. Akimoto and H. Iwahara, *Solid State Ionics*, 1993, **67**, 71.
2 N. Kundsen, E. K. Anderson, I. G. K. Anderson, P. Norby and E. Skou, *Solid State Ionics*, 1993, **61**, 153.
3 (*a*) I. Ichinose, H. Senzu and T. Kunitake, *Chem. Mater.*, 1997, **9**, 1296; (*b*) Y. Aoki and T. Kunitake, *Adv. Mater.*, 2004, **16**, 118; (*c*) Y. Aoki and T. Kunitake, *Chem. Mater.*, 2005, **17**, 450.
4 D. Hausmann, J. Becker, S. Wang and R. G. Gordon, *Science*, 2002, **298**, 402.
5 A. Douy, *J. Eur. Ceram. Soc.*, 2006, **26**, 1447.
6 H. Li and T. Kunitake, *Chem. Lett.*, 2006, **35**, 640.
7 P. Jasinski, V. Petrovsky, T. Suzuki, T. Petrovsky and H. U. Anderson, *J. Electrochem. Soc.*, 2005, **152**, A454.
8 B. C. H. Steele and A. Heinzel, *Nature*, 2001, **414**, 345.
9 (*a*) T. Schober, *Ionics*, 2006, **12**, 131; (*b*) M. Nogami and Y. Abe, *Phys. Rev. B: Condens. Matter*, 1997, **55**, 12108.
10 (*a*) A. Matsuda, T. Kanzaki, Y. Kotani, M. Tatsumisago and T. Minami, *Solid State Ionics*, 2001, **139**, 113; (*b*) A. Matsuda, T. Kanzaki, Y. Tadanaga, M. Tatsumisago and T. Minami, *J. Ceram. Soc. Jpn.*, 2002, **110**, 131.
11 M. Nogami, K. Miyamura and Y. Abe, *J. Electrochem. Soc.*, 1997, **144**, 2175.
12 H. Iwahara, T. Shimura and H. Matsumoto, *Electrochemistry*, 2000, **68**, 154.
13 G. Connell and J. A. Dumesic, *J. Catal.*, 1987, **105**, 285.
14 (*a*) C. E. Bronnimann, R. C. Zeigler and G. E. Maciel, *J. Am. Chem. Soc.*, 1988, **110**, 2023; (*b*) C. E. Bronnimann, I.-S. Chuang, B. L. Hawkins and G. E. Maciel, *J. Am. Chem. Soc.*, 1987, **109**, 1562.
15 I. Kosacki and H. U. Anderson, *Appl. Phys. Lett.*, 1996, **69**, 4171.
16 N. Ito, M. Iijima, K. Kimura and S. Iguchi, *J. Power Sources*, 2005, **152**, 200.
17 (*a*) M. Hashizume and T. Kunitake, *Langmuir*, 2003, **19**, 10172; (*b*) M. Hashizume and T. Kunitake, *Soft Matter*, 2006, **2**, 135.